Clinical Epigenetics

RESEARCH

Open Access

Distinct methylome profile of cfDNA in AMI patients reveals significant alteration in cAMP signaling pathway genes regulating cardiac muscle contraction

Manoswini Dash[1,2], Bhawna Mahajan[1,3*], Shobhita Shah[1], Ghulam Mehdi Dar[1], Parameswar Sahu[1], Abhay Kumar Sharma[1], Nimisha[1] and Sundeep Singh Saluja[1,4]

Abstract

Background The role of epigenetics in cardiovascular diseases has paved the way for innovative therapeutic approaches. Investigating epigenetic changes using cell-free DNA (cfDNA) holds substantial promise beyond mere diagnostics, especially for heart-related conditions like acute myocardial infarction (AMI), where obtaining tissue samples is a challenge. This study explores the methylation patterns of cfDNA in AMI patients and compares them with genomic DNA (gDNA) from the same individuals, aiming to evaluate the effectiveness of cfDNA as a valuable resource for studying heart-related diseases.

Methodology We generated global methylome profiles of cfDNA and gDNA from 25 AMI patients using EM-Seq. Tissue deconvolution analysis was performed to estimate tissue specificity based on the methylation patterns. Differentially methylated loci were identified and explored to understand AMI pathophysiology.

Results Comparative analysis of cfDNA and gDNA methylation patterns in AMI patients reveals cfDNA holds more significance than gDNA. Principal component analysis revealed distinct clusters for cfDNA and gDNA, indicating distinct methylome profiles. cfDNA originated from multiple sources, predominantly from neutrophils (~75%) and about 10% from the left atrium, highlighting cardiac-specific changes. In contrast, immune cells are the major source of gDNA, indicative of inflammatory responses. Gene set enrichment analysis (GSEA) associates cfDNA methylation patterns with pathways related to cardiac muscle contraction, inflammation, hypoxia, and lipid metabolism. The affected genes include G protein-coupled receptors (GHSR, FFAR2, HTR1A, and VIPR2) that are part of the cAMP signaling pathway.

Conclusion Epigenetic changes in cfDNA are more specific to cardiac tissue compared to those in gDNA, providing better insights into the molecular mechanisms involved in AMI. Genes that are differentially methylated in cfDNA and regulate core pathways, such as cAMP signaling, could be targeted for clinical applications, including the development of effective biomarkers and therapeutic targets.

Keywords Cell-free DNA, Acute myocardial infarction, Tissue specificity, Epigenetics, EM-seq, Methylome sequencing

*Correspondence:
Bhawna Mahajan
drbhavna.gbph@nic.in
Full list of author information is available at the end of the article

Background

Cardiovascular diseases (CVDs) that include maladies of blood and vessels continue to be the leading cause of global mortality. In 2021, CVDs claimed the lives of 20.5 million people, about one-third of the global deaths [1]. Low- and middle-income countries are facing a heavy CVD burden, contributing to 4 out of 5 CVD-related deaths [2]. Ischemic heart disease or coronary artery disease (CAD) is the atheromatous changes in the coronary artery that supply blood to the heart, representing a majority (9.1 million in 2019) of CVD-associated fatalities [3]. The progression of CAD predominantly reduces coronary blood flow, leading to inadequate oxygen delivery to the heart cells. This ultimately leads to irreversible myocardial necrosis, commonly known as an acute myocardial infarction (AMI) or heart attack [4]. With advancements in medicine and awareness, it is postulated that up to 80% of premature heart diseases and 75% of recurrent cardiovascular events can be prevented [5]. Such progress can be made by understanding the contributory modifiable and non-modifiable risk factors. Although risk factors for CAD are known to change significantly with ethnicity [6], environment [7], and lifestyle [8], where 40–60% of CAD cases are explained by their genetic component [9], the remaining half may be justified by gene–environment interactions or epigenetics [10]. In the past few decades, the involvement of epigenetics has been acknowledged and studied extensively in CAD [11]. Epigenetics includes heritable and reversible modifications of the DNA without change in the genetic sequence, which can alter the functioning and expression of the genes crucial in pathogenesis. Epigenetic alterations include methylation, histone modifications, chromatin remodeling, and miRNA regulation [12]. Shi et al., and Sumi et al., have broadly summarized the epigenetic landscape of cardiovascular and coronary artery diseases [13, 14]. DNA methylation is a key epigenetic modification actively involved in regulating gene expression. Numerous studies have focused on elucidating methylation patterns to unveil the gene regulation in myocardial infarction patients using blood-derived genomic DNA [15–17]. Although the limitation on the availability of AMI heart tissue is well understood, studying blood cells-derived genomic DNA (gDNA) might not completely reflect the methylation alterations in cardiac cells. An alternative to address this limitation could involve analyzing cell-free DNA (cfDNA) obtained from the blood of AMI patients, potentially originating from the necrotized cardiomyocytes [18]. The principle behind the concept is that during pathology, tissues undergoing apoptosis and necrosis actively release the fragmented DNA into the circulation [19]. Therefore, provided that confounding factors like other potential sources of cfDNA are excluded, cfDNA might reflect the actual state of the tissue under study [20]. Recently, methylation patterns have been utilized to determine tissue specificity and identify the source of cfDNA, presenting a novel approach to studying tissue pathogenesis [21, 22].

Although there are distinct studies investigating methylation differences in AMI patients from healthy adults by using either gDNA or cfDNA, there is a lack of research demonstrating the similarities or differences in methylation patterns based on the source, within AMI patients. Secondly, there are controversies regarding the tissue specificity of the cfDNA [23] that need to be addressed before considering cardiomyocyte-derived cfDNA as a surrogate tissue to study AMI. Therefore, to determine whether cfDNA accurately reflects the condition of cardiac tissue and carries unique methylation signatures, it should exhibit distinct methylation patterns compared to those found in the blood tissue of the same individual. It will strengthen the argument that cfDNA is indeed representative of diseased cardiac tissue and establish the validity of using cfDNA as a biomarker for cardiac conditions. To address this, we compared the global methylome pattern of cfDNA and gDNA from AMI patients, aimed at establishing the significance of methylation changes between them.

Methodology

Sample collection

Patients with suspected AMI at the emergency department of Govind Ballabh Pant Institute of Postgraduate Medical Education and Research (GIPMER), New Delhi, India, underwent detailed evaluation including medical and family history, clinical examination, demographic details, ECG, and cardiac biomarker assessment. Those with confirmed AMI within 24 h of onset of the symptoms were included in the study. All patients included in the study provided their informed written consent after receiving comprehensive information about the study and its objectives. No healthy adults were included as controls in this study, as the aim was to observe methylation changes within AMI patients using two different sources of DNA. Around 10 ml of peripheral blood was collected from each patient. Figure 1a summarizes the inclusion/exclusion criteria, distribution, and utilization of the blood samples for biochemical and molecular processing. Samples that failed to achieve the threshold quality, quantity, fragment size, and purity for methylome library preparation were excluded. The study was approved by the Institute ethics committee (IEC/MAMC/(75/03/2020/No:116)) of MAMC, New Delhi.

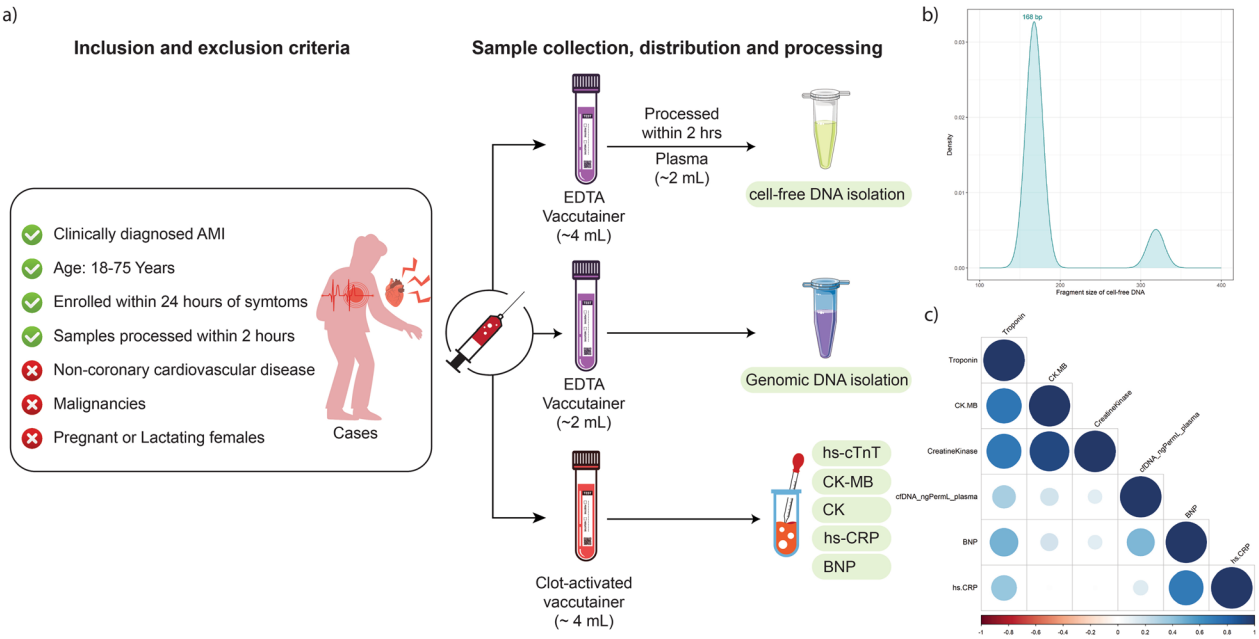

Fig. 1 Conceptual schema and methodology for sample processing. **a** Diagrammatic representation of inclusion and exclusion criteria with the distribution and processing of the collected blood sample. **b** Bioanalyzer-derived fragment size with an average fragment of 167.72 bp (range: 100–200 bp). **c** Correlation between cardiac biomarkers and cfDNA

Biochemical profiling

Around 2 ml of serum was used for cardiac biomarker profiling. The serum levels of high-sensitivity troponin T (hs-TropT) and brain natriuretic peptide (BNP) were measured by electrochemiluminescence on Elecsys e411 (Roche Diagnostics, Manheim, Germany). Meanwhile, creatine kinase-myocardial band (CKMB), creatine kinase (CK-T), and high-sensitivity C-reactive protein (hs-CRP) were measured on fully automated autoanalyzer c501 using commercially available kits from Roche Diagnostics, Manheim, Germany.

cfDNA and gDNA isolation

To achieve maximum quantity and quality, plasma separation was performed within two hours of sample collection. The isolation process involved two-step centrifugation, first at 2000 g for 10 min, followed by 16,000 g for 10 min, both performed at 4 °C. The plasma samples were either stored at − 80 °C or processed immediately for cfDNA isolation using the MagMAX™ cell-free DNA isolation kit (Cat. No. A29319, Thermo Fisher Scientific), following the manufacturer's protocol. To maximize DNA recovery, the cfDNA was stored in LoBind tubes (Cat. No. 0030108418, Eppendorf). Approximately 300 uL of whole blood was processed for genomic DNA extraction using the Promega genomic DNA isolation kit. The cfDNA and gDNA were quantitatively and qualitatively assessed by agarose gel electrophoresis (only for gDNA), spectrophotometry (Nanodrop, ThermoScientific, USA) analysis to ascertain purity, fluorometry (Qubit 3.0 DNA dsDNA high-sensitivity Assay Kit from Life Technologies, Carlsbad, CA) for nucleotide quantification, automated electrophoresis assay using the 2100 Bioanalyzer with high-sensitivity DNA chips (Agilent Technologies, Santa Clara, CA) to assess fragment size of cfDNA and detect the presence of any genomic DNA contamination. Samples within acceptable 260/280 ~ 1.8 and with DNA quantity between 10 and 200 ng were considered for methylome library preparation. Similarly, the cfDNA samples that met the quality (260/280 ~ 1.8, no gDNA contamination, fragment size range 160–200 bp) and quantity (cfDNA > 20 ng) were selected for the methylome library preparation.

Global methylome sequencing using enzymatic-conversion (EM-Seq)

Considering its natural fragmentation, the cfDNA isolated from AMI patients were excluded from shearing. Mechanical shearing of gDNA was performed using Covaris ME220-focused ultrasonicator, matching the cfDNA fragment length. The input gDNA (ranging from 10 to 200 ng) was sheared in a microTUBE-50 AFA Fiber Strip V2, with peak power (W) at 50, duration (s) at 214, duty factor (%) at 30, and cycles per burst (#) at 1000. The DNA fragments were then assessed in Agilent

Bioanalyzer 2100 Systems using a high-sensitivity DNA (hsDNA) kit.

The whole-genome methylation library was prepared using NEBNext® Enzymatic Methyl-seq (EM-seq™) kit, following the manufacturer's instructions on selected samples using 100 ng of cfDNA and gDNA. This kit employs an enzyme-based method known for its high performance as an alternative to the whole-genome bisulfite sequencing (WGBS) approach. Notably, EM-seq provides advantages when working with samples with minimum DNA quantity. Briefly, this method employs the Ten-eleven translocation 2 (TET2) enzyme and an oxidation enhancer to catalyze the oxidation of 5-mC and 5-hmC to 5-carboxycytosine (5caC) [24]. This process serves the dual purpose of safeguarding these modified bases from deamination by the APOBEC3A enzyme in the subsequent step, wherein unmethylated cytosines undergo deamination, ultimately converting to uracil. The library was spiked in with methylated pUC19 and unmethylated lambda as control. The captured library was quantified by Qubit fluorometer followed by the quality check and size distribution using Agilent Bioanalyzer 2100 system high-sensitivity DNA kit. EM-seq libraries for each sample were individually prepared with dual indexing and then sequenced on the NextSeq 2000 (Illumina, USA) using NextSeq 2000 P3 Reagents (300 Cycles) v3, with a minimum sequencing depth of 100 M reads per sample.

Bioinformatics analysis of methylome data

The high-throughput sequencing generated paired-end reads with 150 bp read length. Raw data quality was checked using FastQC v0.11.9. Low-quality reads were removed, and adapters trimming was done using Trimmomatic v0.39 with the specified parameter [Trimmomatic-0.39/adapters/TruSeq3-PE.fa:2:30:10 LEADING:20 TRAILING:20 SLIDINGWINDOW:4:15 MINLEN:35]. The reads were mapped to the GRCh38.p13 human reference genome and control sequence (phage lambda, puc19c) using the GEM3 mapper. Methylation calling for all genomic cytosines, was carried out using BS-call, a component of the GemBS v4.0.4 package, in both CpG and non-CpG contexts [25]. The GemBS output files (bed files) were imported to methylKit (version 1.26.0) using R for further analysis [26]. The methylation status of a base with a minimum 5× coverage was used to identify differentially methylated regions (DMRs). The methylation values were filtered, normalized, merged, and processed following a tiling window model (500 bp sliding window with step size 500). The significance of DMRs (p-value) was estimated by Fisher's exact test, and *q*-values calculated, following SLIM algorithm. The tiling window with methylation difference greater than 10 and q value < 0.01 was further annotated using a genomation package [27]. The distribution of differential methylation across the genome was estimated for both cfDNA and gDNA (promoter, exon, intron, intergenic, 5` and 3` UTRs). Further annotation was performed using CHIPseeker [28]. Gene ontology, enrichment, and pathway analysis (using the KEGG database) on selected DMRs were carried out using clusterProfiler and [29] ShinyGo R packages [30].

Tissue deconvolution analysis

It is believed that the primary sources of cfDNA in cases of AMI are inflammatory and cardiomyocyte cells that necrotize because of low oxygen levels. To ensure the tissue of origin of cfDNA, the methylome data were deconvoluted using a human methylome reference atlas consisting of 25 human cell types [31]. Utilizing the BSmeth2Probe function within deconvR [32], methylation data were mapped to CpG probe IDs, facilitating the deconvolution of WGBS cfDNA samples into their respective cell types of origin.

Results

A total of 25 AMI patients were selected for the study, with a mean age of 52.12 ± 2.39 years that included 22 males (88%, 51.13 ± 2.65 years) and three females (12%, 59.33 ± 0.66 years). Around 44% of the patients fall into the young adult category (below 55 years) and are classified as experiencing AMI in young adults (Table 1). The patients diagnosed with ST-elevation myocardial infarction (STEMI) exhibited elevated levels of hs-cTnT and other classical cardiac-specific markers like CK-MB, CK, hs-CRP, and BNP (Table 1).

Besides cardiac-specific biomarkers, we have measured biochemical parameters known to be associated with AMI and examined the correlation between cfDNA concentration and these parameters. The concentration of cfDNA has shown a positive yet insignificant correlation with BNP and a weak correlation with hs-cTnT and CK-MB (Fig. 1c). Based on the fluorometry assay (Qubit 3.0), the amount of cfDNA obtained from the AMI patients ranged from 3.84 to 33 ng per mL of plasma, with a mean of 7.87 ± 1.32 ng/mL. Fragment analysis of cfDNA has shown uniformity in the fragment size with an average fragment of 167.72 bp (range: 100–200 bp) (Fig. 1b).

Contrasting methylation profiles of cfDNA and gDNA in AMI patients

The average global methylation level of cfDNA and gDNA in AMI patients was comparable and found to be in a range of 60–70% (Fig. 2a). However, the distribution of percentage methylation in terms of methylation status

Table 1 Demographic features, clinical characteristics, and risk factor information of the study subjects

Parameters	Subjects ($n=25$)
Gender	
Males	22 (88%)
Females	3 (12%)
Age	52.12 ± 11.98
Males	51.13 ± 12.46
Females	59.33 ± 1.15
Young AMI (≤ 55)	11 (44%)
Old AMI (> 55)	14 (56%)
Socio-economic status	
Good	13 (52%)
Moderate	3 (12%)
Poor	9 (36%)
Clinical symptoms	
Dyspnea	23 (92%)
Palpitation	16 (64%)
Syncope	8 (32%)
Vomiting	13 (52%)
Risk factors	
Obesity	12 (48%)
Tobacco	3 (12%)
Alcohol	4 (16%)
Family history	6 (24%)
Diet (non-vegetarian)	10 (40%)
Comorbidity	
No comorbidity	9 (36%)
Diabetes	13 (52%)
Hypertension	11 (44%)
Diabetes and hypertension	8 (32%)
Biochemical assays	
hs-cTnT (< 0.001 ng/mL)	11.74 ± 12.81
CK-MB (5–25 U/L)	307.28 ± 358.70
CK (22–198 IU/L)	2995.08 ± 2751.41
hs-CRP (1–3 mg/dL)	21.62 ± 25.76
BNP (0–124 pg/mL)	3317.14 ± 3400.11
Molecular assays	
cfDNA (ng/uL)	5.08 ± 3.52
gDNA (ng/uL)	460.63 ± 327.01

reveals that hypermethylation is more abundant in both the cfDNA and gDNA. While complete methylation is relatively higher in gDNA, cfDNA has more partial methylation (Fig. 2b). The distribution of the differential methylation across genomic regions showed its abundancy in intronic and intergenic regions. While the exon has higher differential methylation in gDNA, cfDNA showed a higher percentage of differential methylation in the promoters (Fig. 2c). Principal component analysis (PCA) reveals distinct methylation patterns between cfDNA and gDNA, indicating differences in the methylome of cfDNA compared to gDNA among AMI patients (Fig. 2d).

Heterogeneous origin of cfDNA with immune cells and cardiomyocytes as major sources

During MI, cardiomyocytes in areas deprived of oxygen die by both apoptosis and necrosis, releasing cellular content with fragmented DNA into the bloodstream [33]. To ascertain the origin of cfDNA and quantify the contribution of different cell types, methylation-based cell-type deconvolution was performed by comparing the methylation patterns with a comprehensive human methylome reference atlas [31], which encompasses 25 human cell types. Neutrophils are found to be the major cell types in cfDNA (~75%) along with erythrocyte progenitor cells (20%) (Fig. 3a, b). We also observed that the left atrium and monocytes contribute to the total cfDNA, each with around 10%. cfDNA from other cell types like cortical neurons, hepatocytes, NK-cells, and CD4 and CD8 cells is also seen (Fig. 3a, b). However, for gDNA, neutrophils and monocytes are the major cell types (Fig. 3a). To further stratify, we investigated the cell type contribution in each sample (Fig. 3c). Patients whose cfDNA originates from cell types other than cardiomyocytes, such as hepatocytes, lung cells, pancreatic acinar cells, or cortical neurons, tend to have minimal or reduced levels of cardiac-origin cfDNA (Fig. 3c), which implies that the source of cfDNA extends beyond cardiomyocytes in AMI patients.

DMRs exhibit uniqueness within the cfDNA of AMI patients

The methylome profile generated from blood tissue primarily reflects methylation patterns from blood cells. Comparing it with the cfDNA methylome isolated from blood will help to assess whether analyzing cfDNA provides any additional insights or differences compared to analyzing methylome profiles directly from blood samples. To explore the differences in methylation patterns between cfDNA and gDNA, we analyzed samples for which methylome data were generated from both sources ($n=14$). A total of 679 DMRs (each of length 500 bp) were obtained. Additional filtration and data cleaning yielded 623 DMRs (supplementary file 1). Among these, 218 (35%) are hypermethylated and 405 (65%) hypomethylated, and these DMRs are distributed across various genomic regions, including promoters (3000 bp flanking the TSS), 5' UTRs, 3' UTRs, gene bodies, and intergenic regions (Fig. 4a). The majority of DMRs are located within gene bodies (38.8%), followed by intergenic regions (32.6%), promoters (20.7%), and untranslated regions (UTRs) (7.9%) and hypomethylation is notably more prevalent (Fig. 4b). DMRs are more abundant

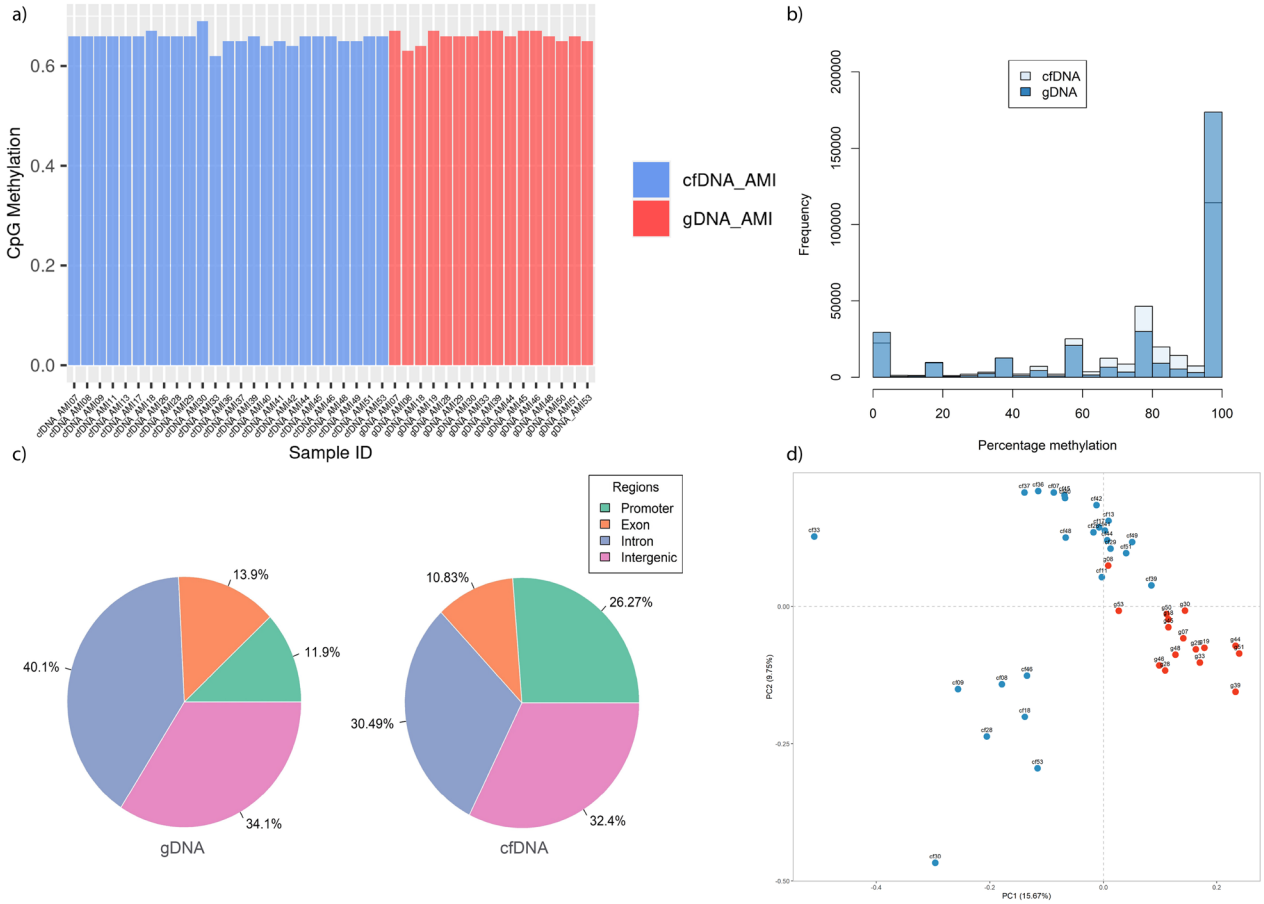

Fig. 2 Genome-wide distribution of methylation estimated from cell-free DNA and genomic DNA of AMI patients **a** average percentage methylation estimated from cfDNA and gDNA of AMI patients. The panel shows the mean methylation levels for cfDNA and gDNA of all samples ($n=25$), **b** histogram for percent methylation distribution from the total cfDNA and gDNA of matched control ($n=25$), **c** proportion of methylated regions in various genomic contexts (e.g., promoter, exon, intron) between cfDNA and gDNA, highlighting differences in methylation patterns between these two DNA sources ($n=25$), **d** PCA plot depicting the clustering of cfDNA and gDNA methylation patterns ($n=25$). Each point represents a sample, with clusters indicating similarities in methylation profiles

in proximity to the transcription start site (TSS) (11%) compared to the gene body and flanking regions (Fig. 4c). Within the gene body, most of the DMRs were situated within the intronic regions of the genes, while those within the exonic regions tended to be predominantly located toward the downstream exons. We also showed the chromosome-wide distribution of differential methylation (Fig. 4d).

Differential methylation in and around promoters of protein-coding loci

The role of methylation in the promoter region holds greater significance in regulating the expression of neighboring genes compared to the debated role of gene body methylation [34]. This distinction arises from the multifaceted nature of gene body methylation, which impacts transcription rates and governs alternate splicing [35], histone methylation, and maintains transcription fidelity by preventing the production of erroneous transcripts [36, 37]. To make a meaningful interpretation, we categorized differentially methylated regions (DMRs) and associated genes into two groups based on their presence in the promoter or gene body. Initially, we focused on the DMRs located within and around the promoter and then further filtered the data based on three criteria: (i) their association with myocardial infarction according to the CTD database, (ii) methylation difference greater than 25, and (iii) genes were protein coding. Among the 129 genes identified to have DMRs in and around promoters in our study, 73 are known to be associated with myocardial infarction as per the CTD database, of which 41 loci with methylation differences exceeding 25 (Table 2).

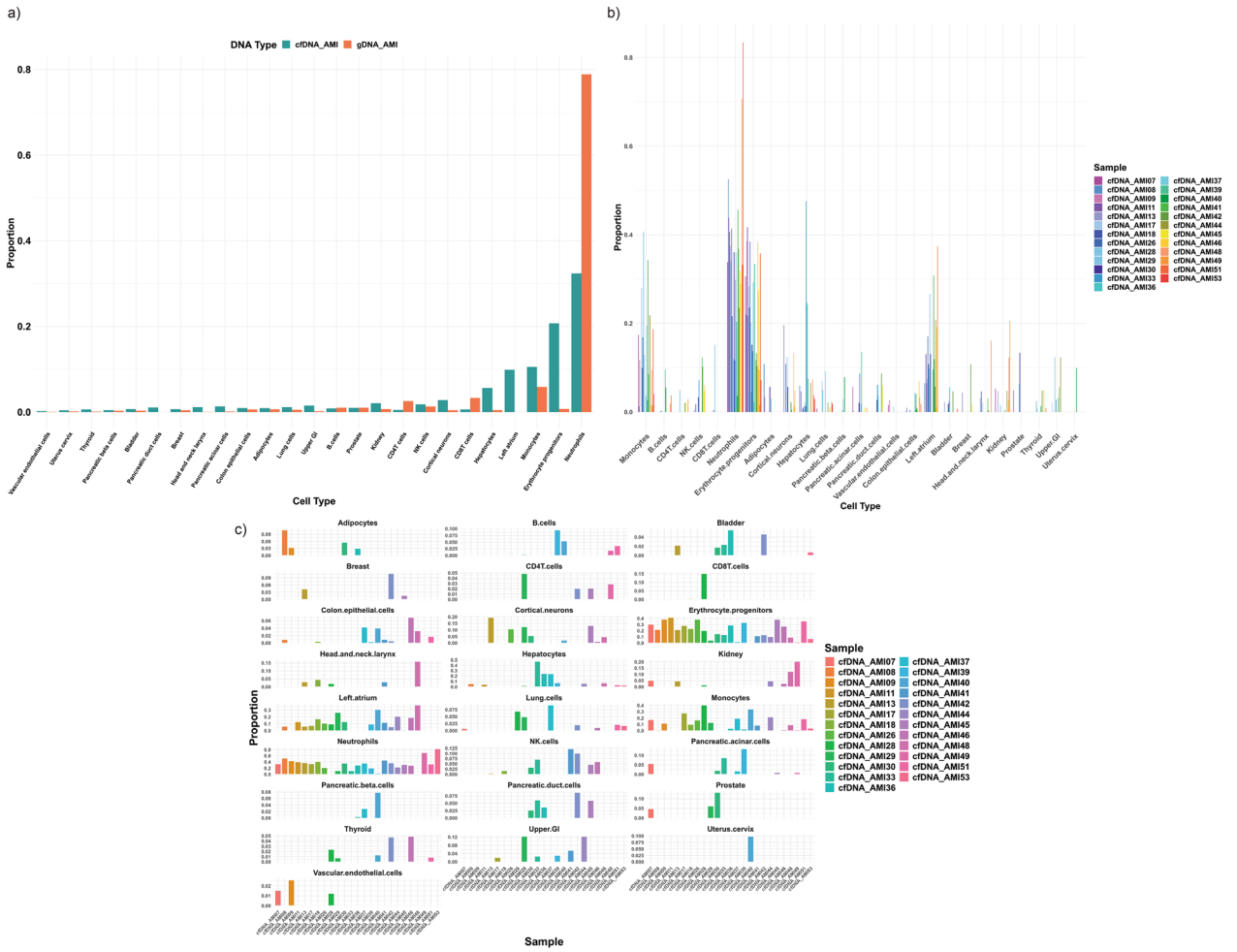

Fig. 3 Tissue-type deconvolution from methylation data in cfDNA and gDNA of AMI patients. **a** Tissue-type distribution of cfDNA from AMI patients, **b** average of tissue specificity across cfDNA and gDNA comparison of cell-type between cfDNA and gDNA, **c** samplewise analysis of tissue specificity showing the source of cfDNA

Gene set enrichment analysis revealed altered methylation in hypoxia and cardiac muscle contraction-related pathways

The list of genes associated with DMRs was identified by annotating the DMRs (supplementary file 2). The gene set enrichment analysis (GSEA) was performed using clusterProfiler that ranked the genes obtained from the study [29]. These genes were used to identify the affected pathways with their level of significance and adjusted for multiple hypothesis testing (supplementary file 3). Several pathways were identified, predominantly associated with the inflammatory response, calcium signaling, hypoxia response, as well as lipid and carbohydrate metabolism. Figure 5 shows the enrichment distribution and list of genes associated with the major pathways. The genes associated with the most relevant and significant pathways are shown in network plots (Fig. 6). Additionally, based on the pathway enrichment results we found cAMP signaling and cardiac muscle contraction as two most significantly differentially methylated pathways. A brief and relevant KEGG-based outline of these pathways and their respective differentially methylated genes are illustrated in Fig. 7.

Epigenetic alterations in cAMP signaling receptors govern critical cardiac functions.

The cAMP signaling pathway is critical in the physiological response to acute myocardial infarction (AMI), influencing various processes such as vascular tone, cardiac contractility, inflammation, and cell survival. In our study, several genes related to the cAMP signaling pathway exhibited significant differential methylation in the cfDNA of AMI patients. These genes, including ADCY9, GHSR, FFAR2, GRIN2D, HTR1A, PPARA, BDNF, SLC9A1, TIAM1, and VIPR2, are involved in processes such as remodeling of vascular endothelial

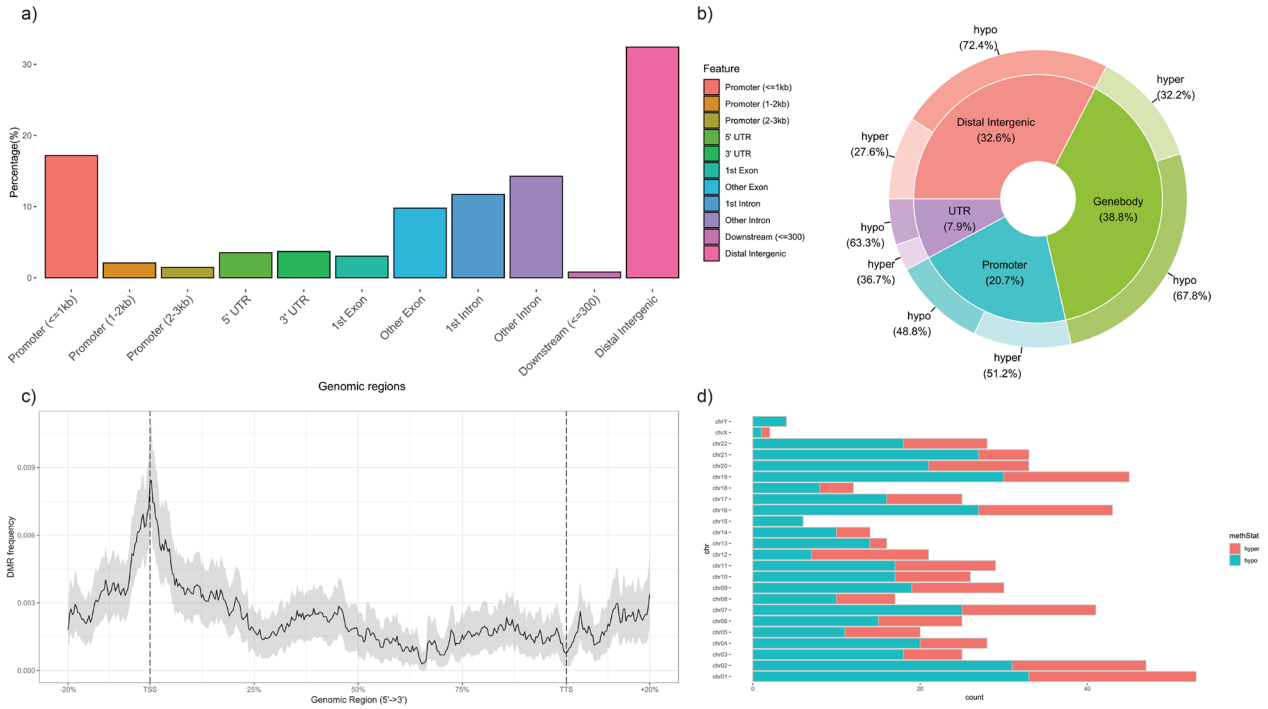

Fig. 4 Genome-wide distribution of DMRs. **a** Distribution of DMRs in genomic regions like promoter, gene body (exon and intron), UTRs, and distal intergenic regions. **b** Methylation status of the DMRs in different genomic regions. **c** Average distribution of DMRs showing relatively higher DMRs around TSS. **d** Chromosome-wide distribution of DMRs and their methylation status

cells, apoptosis, fatty acid oxidation, calcium signaling, and cardiac muscle contraction via the cAMP signaling pathway (Fig. 7). It is intriguing to note that many of the epigenetically modified loci are G protein-coupled receptor (GPCR) proteins (GHSR, FFAR2, HTR1A, and VIPR2), which bind to ligand molecules and play a role in regulating various downstream processes via the cAMP-signaling pathway, which are inherently linked to cardiovascular conditions.

Discussion

cfDNA offers more than just diagnostic and management benefits—its role in treatment decision-making and as a therapeutic biomarker is also well-evidenced [38]. Recent studies have focused on investigating various features of cfDNA, including its quantity in blood and other body fluids, fragment size, and half-life, and their associations with disease conditions. While cfDNA holds significant potential, its application has been limited to a few disease models, notably cancer and autoimmune disorders. In cancers, circulating cfDNA (also known as ctDNA) is being extensively studied to be used as a modality for minimally invasive liquid biopsy to replace solid biopsy [39]. However, its role is crucial in diseases affecting visceral organs, particularly in cases where obtaining tissue samples is challenging. One of the recent applications is the use of donor-derived cfDNA as a diagnostic tool for transplantations is under progress [40–42].

The application of cfDNA in heart-related diseases holds particular importance. Our earlier study (under communication) found that cfDNA is around 14 times higher in AMI patients than in healthy adults. The tissue specificity attribute of methylation is widely recognized, and existing literature indicates a significant difference in methylation patterns between the heart tissues of AMI patients and those of healthy adults, contributing to the disease progression. Tan et al. [43] have summarized the studies that have explored cfDNA as a potential early diagnostic and prognostic marker in AMI. Consistent with the applications of cfDNA, a few studies [44–47] have explored the methylation differences in AMI patients using their plasma-derived circulating cell-free DNA. In this study, we posed the question: Does cfDNA manifest tissue-specific methylation patterns in AMI patients, specifically reflecting cardiac specificity? Furthermore, we explored whether these variations are distinct enough to distinguish them from the methylation patterns of other cell types found in the bloodstream. To investigate, we compared the cfDNA and gDNA from the same AMI patients. The hypothesis was that if cfDNA demonstrates discernible methylation distinctions from other blood cells and reflects tissue specificity, it could

Table 2 List of genes differentially methylated in the promoter region with their methylation status, genomic annotation, methylation difference, and significance

Symbol	Chromosome	DMR_start	DMR_end	Methylation difference	*q*value	Methylation status	Genomic annotation
TTBK1	Chr6	43,243,001	43,243,500	−72.74	5.71E-15	Hypo	Within TSS
SALL1	Chr16	51,151,001	51,151,500	−67.04	2.37E-15	Hypo	Within TSS
DNMT3A	Chr2	25,252,501	25,253,000	−57.11	1.29E-05	Hypo	Promoter (< = 1 kb)
LDLRAD4	Chr18	13,641,501	13,642,000	−49.89	1.00E-08	Hypo	Within TSS
PNMA2	Chr8	26,513,501	26,514,000	−47.06	9.83E-07	Hypo	Within TSS
RESP18	Chr2	219,331,501	219,332,000	−41.28	6.03E-06	Hypo	Promoter (< = 1 kb)
PPP1R14A	Chr19	38,256,001	38,256,500	−40.95	1.65E-06	Hypo	Within TSS
RTKN	Chr2	74,442,001	74,442,500	−40.77	8.77E-06	Hypo	Promoter (< = 1 kb)
ELAVL2	Chr9	23,821,001	23,821,500	−40.15	0.002342299	Hypo	Within TSS
ASPG	Chr14	104,085,501	104,086,000	−40.00	0.005863143	Hypo	Within TSS
KLK7	Chr19	50,984,001	50,984,500	−38.50	4.84E-05	Hypo	Within TSS
STEAP1	Chr7	90,153,501	90,154,000	−36.54	7.53E-05	Hypo	Promoter (< = 1 kb)
HOXC5	Chr12	54,031,501	54,032,000	−36.44	0.004658024	Hypo	Promoter (1-2 kb)
MIR208B	Chr14	23,418,001	23,418,500	−35.48	0.00010589	Hypo	Within TSS
OLIG3	Chr6	137,494,501	137,495,000	−34.62	0.000165504	Hypo	Promoter (< = 1 kb)
HTR1A	Chr5	63,962,501	63,963,000	−32.00	0.000306617	Hypo	Promoter (< = 1 kb)
TPM2	Chr9	35,693,001	35,693,500	−30.80	0.007318167	Hypo	Promoter (2-3 kb)
FGFR2	Chr10	121,597,001	121,597,500	−28.70	0.000494675	Hypo	Promoter (< = 1 kb)
SFTPD	Chr10	79,983,001	79,983,500	−27.50	0.000225499	Hypo	Promoter (< = 1 kb)
TMEM88B	Chr1	1,425,501	1,426,000	−26.76	2.28E-05	Hypo	Within TSS
CRMP1	Chr4	5,890,501	5,891,000	−26.14	7.65E-05	Hypo	Promoter (< = 1 kb)
PHACTR3	Chr20	59,583,501	59,584,000	−25.00	1.71E-05	Hypo	Within TSS
TMEM176B	Chr7	150,801,001	150,801,500	25.71	2.11E-05	Hyper	Within TSS
EPS8	Chr12	15,789,501	15,790,000	26.20	0.000585189	Hyper	Promoter (< = 1 kb)
CBLC	Chr19	44,777,501	44,778,000	28.37	0.008399354	Hyper	Within TSS
ARHGAP36	ChrX	131,082,001	131,082,500	30.00	0.00190226	Hyper	Within TSS
H1-1	Chr6	26,017,501	26,018,000	30.91	3.63E-05	Hyper	Within TSS
FRRS1L	Chr9	109,167,001	109,167,500	31.03	1.81E-06	Hyper	Within TSS
DOK7	Chr4	3,476,001	3,476,500	33.09	0.001766174	Hyper	Within TSS
SRGAP1	Chr12	63,843,001	63,843,500	33.93	0.00895754	Hyper	Promoter (1-2 kb)
CLDN6	Chr16	3,018,501	3,019,000	36.88	0.003000378	Hyper	Promoter (< = 1 kb)
EMILIN3	Chr20	41,367,001	41,367,500	38.10	8.11E-05	Hyper	Promoter (< = 1 kb)
CDH4	Chr20	61,599,501	61,600,000	48.00	6.69E-05	Hyper	Within TSS
GORAB	Chr1	170,531,001	170,531,500	49.50	1.68E-05	Hyper	Promoter (< = 1 kb)
KLK1	Chr19	50,826,501	50,827,000	54.00	0.000165918	Hyper	Promoter (2-3 kb)
GNAL	Chr18	11,751,001	11,751,500	54.53	4.63E-12	Hyper	Within TSS
AUTS2	Chr7	70,693,501	70,694,000	60.61	4.18E-12	Hyper	Promoter (< = 1 kb)
FANK1	Chr10	125,896,501	125,897,000	61.84	2.87E-10	Hyper	Within TSS
DPEP3	Chr16	67,980,001	67,980,500	64.01	4.73E-10	Hyper	Within TSS
CDKL4	Chr2	39,245,001	39,245,500	68.97	7.32E-14	Hyper	Promoter (1-2 kb)
RSPH14	Chr22	23,181,501	23,182,000	69.70	3.33E-17	Hyper	Promoter (< = 1 kb)

serve as a valuable, minimally invasive means to assess cardiac tissue directly. So far, studies have compared the methylome of patients with control using gDNA from blood or heart tissue. To our best knowledge, this is the first study comparing the cfDNA and gDNA obtained from the same resources (i.e., blood of the same AMI patient).

In the proof-of-concept study, we investigated the whole methylome profile from the cfDNA and gDNA of AMI patients, considering gDNA as a matched control.

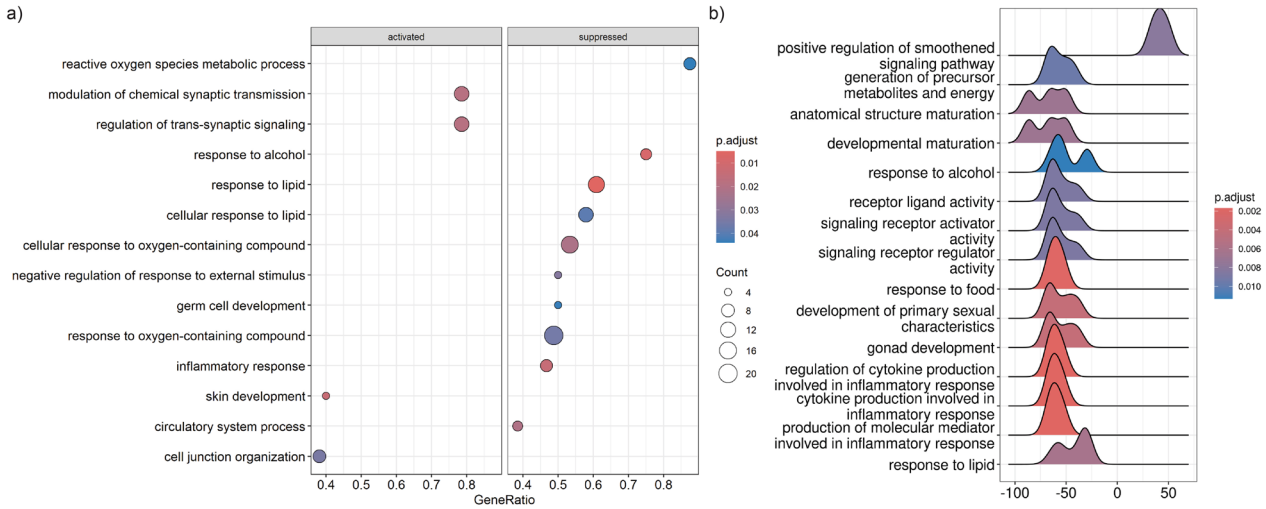

Fig. 5 Gene set enrichment analysis of differentially methylated genes (a) dot plot showing enriched GO terms, (b) ridgeplot visualizing the differential methylation distributions of core enriched genes for GSEA enriched categories

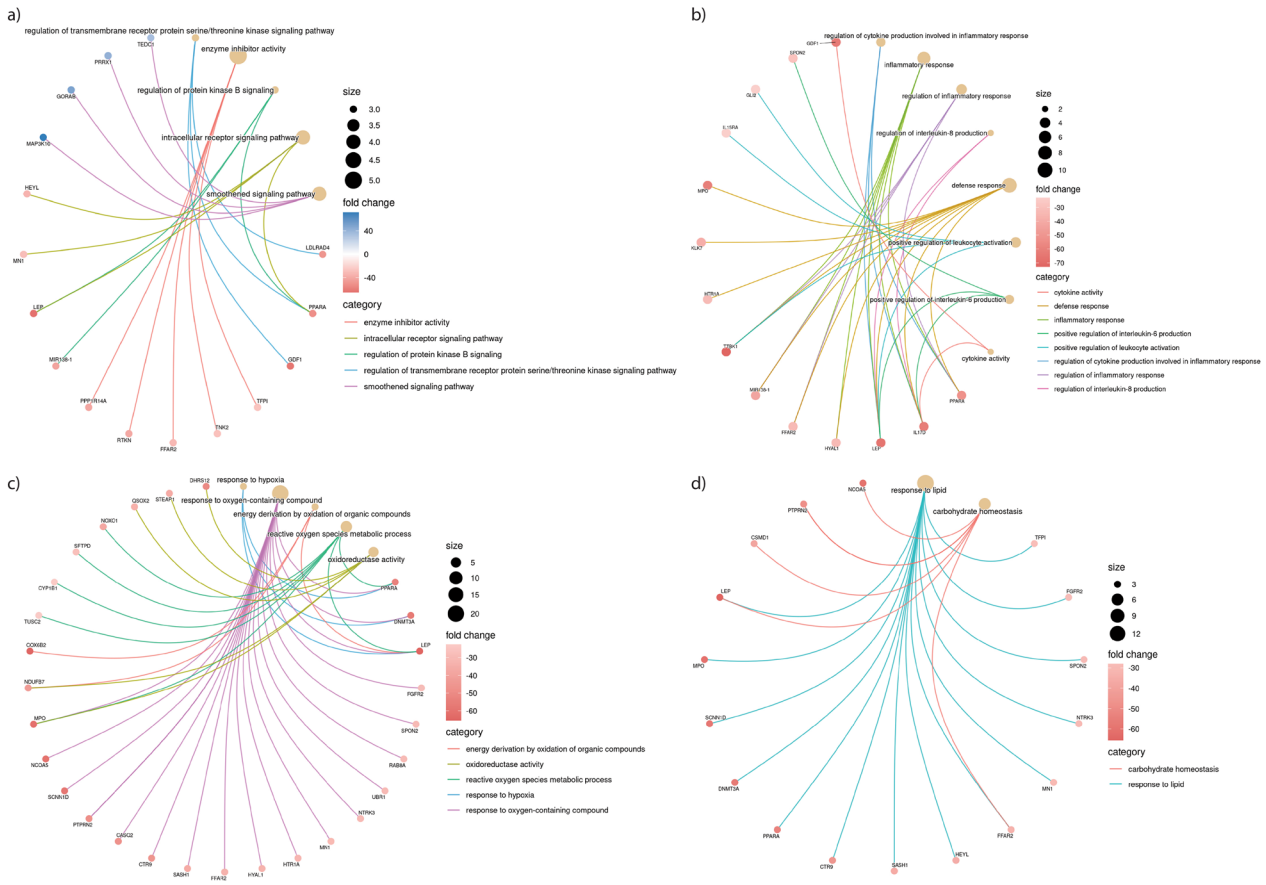

Fig. 6 Network plot showing GO enriched pathways and associated genes **a** signaling pathways, **b** inflammatory response, **c** response to hypoxia, **d** carbohydrate and lipid homeostasis

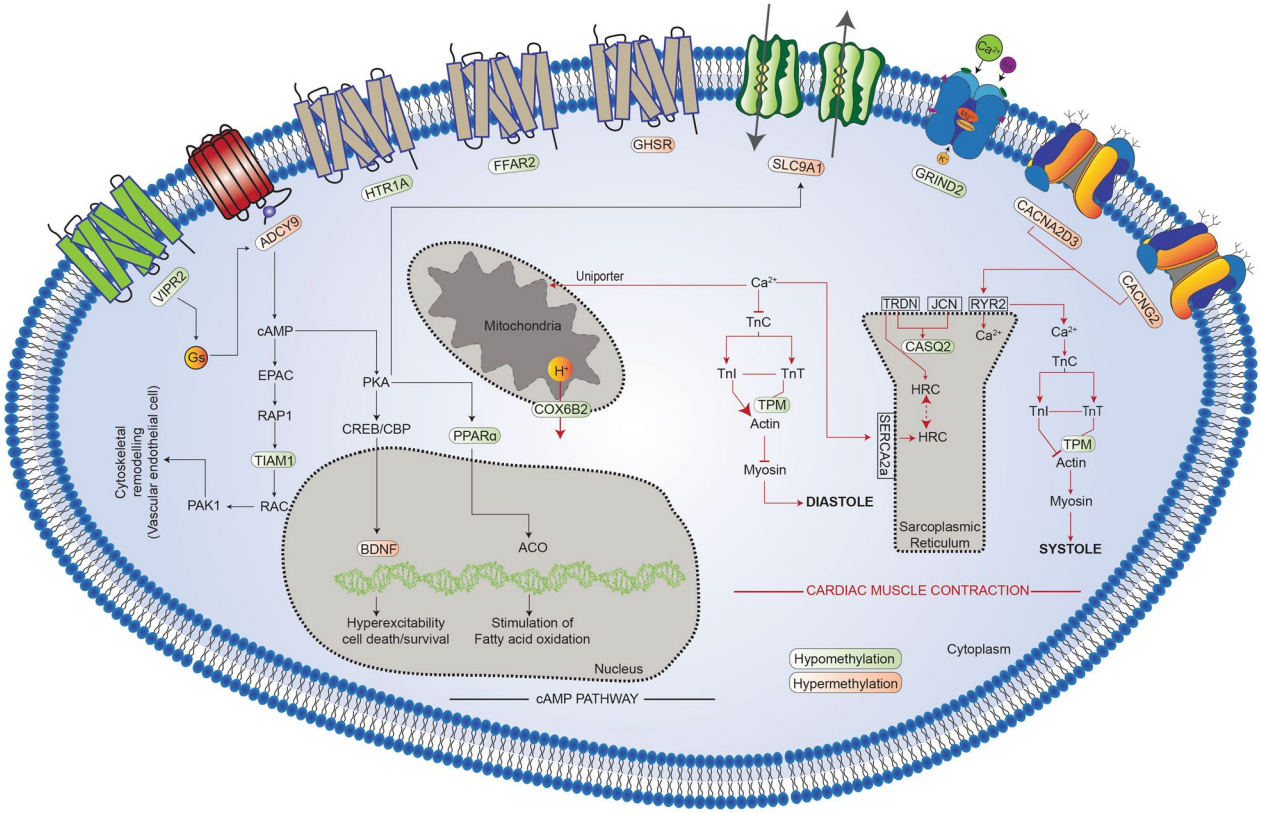

Fig. 7 An illustration of differentially methylated genes (red; hypermethylated, green: hypomethylated) that, based on the pathway enrichment analysis, belong to the two most significant pathways; cAMP signaling pathway (hsa04024) and cardiac muscle contraction pathway (hsa04260)

We intend to underscore the importance of sample processing, as it plays a crucial role in subsequent analyses and outcome. The timing of plasma separation was critical, and we performed it as promptly as possible to prevent contamination from gDNA, and the samples were stored in designated low-retention tubes. As anticipated, we obtained a relatively lower quantity of cfDNA compared to gDNA, and the fragment size of cfDNA, approximately 167 bp—one of the characteristic features of cfDNA—further confirms its origin. We observed a notable difference between cfDNA and gDNA methylome at multiple levels. Although their average methylation levels are similar, they exhibit overall hypermethylation, with variations in the accumulation of differential methylation across genomic regions. Our findings indicate that gDNA methylation patterns, particularly in gene bodies, reflect a general cellular context rather than being specifically tied to diseased states. We found that gDNA exhibits higher gene body methylation, which regulates gene expression through alternative splicing (Shayevitch et al. [35]). Gene body methylation has several implications, primarily in regulating gene expression by maintaining chromatin structure and accessibility, thereby preventing RNA polymerase binding and the formation of spurious transcripts [48]. Moreover, gene body methylation is often conserved across different cell types, contributing to tissue specificity [49]. These observations suggest that the patterns of gDNA methylation represent a broader cellular landscape, providing stability in gene expression rather than reflecting distinct pathological changes. Meanwhile, we observed promoter methylation prominent in cfDNA that plays a key role in transcription silencing and represent a dynamic and reversible regulatory landscape, particularly in response to acute or ongoing physiological changes [50], such as inflammation or tissue injury in our case. Thus, heightened levels in cfDNA may indicate that cfDNA serves as a snapshot of the active epigenetic changes occurring in response to disease processes like AMI. Additionally, based on the methylation pattern, cfDNA forms a different cluster and can be easily distinguishable from gDNA based on the principal component analysis. The distinct clustering of cfDNA based on methylation patterns, as demonstrated by principal component analysis, underscores the unique epigenetic signatures that cfDNA can provide. This differentiation from gDNA not only highlights the

dynamic nature of cfDNA in reflecting physiological and pathological states but also emphasizes its potential as a non-invasive biomarker. The presence and the identification of the potential confounding sources of the cfDNA presents a major challenge in the establishment of the cfDNA as a cardiac-specific biomarker. Our tissue deconvolution analysis of methylome data for cell-type identification consistently identified neutrophils as the primary source for both cfDNA and gDNA. This finding corroborates earlier reports indicating that leukocytes, including neutrophils, are the predominant contributors (70%) to cfDNA levels, regardless of disease status or cfDNA concentration [23, 46]. Neutrophils are the early responders that rush to the ischemic region to clear away dead cell debris. However, excessive accumulation of neutrophils can exacerbate myocardial infarction (MI) by releasing reactive oxygen species (ROS). The subsequent clearance of apoptotic neutrophils by macrophages could potentially contribute to the significant accumulation of neutrophils, which serve as a source of cfDNA [51]. In recent findings, there is compelling evidence pointing to the beneficial role of neutrophils in aiding inflammation resolution and facilitating cardiac repair post-MI. This is achieved through the formation of neutrophil extracellular traps (NETs) and the polarization of macrophages toward a reparative phenotype. Erythrocyte progenitor cells (EPCs) are the second primary source of cfDNA in AMI patients. We found the left atrium as one of the sources for cfDNA, while absent or negligible in the gDNA. The presence of other immune cells like macrophages, monocytes, NK-cells, adipocytes, CD-4, and CD-8 cells can be associated with immune cell infiltration during AMI. The cfDNA originating from adipocytes can be explained by the endocrine and paracrine crosstalk between adipocytes and myocytes. Furthermore, along with adipocyte-originated cfDNA, leptin and other hypoxia-related genes are found to be a differentially methylated point toward the role of adipocyte-mediated cardiac hypertrophy in AMI. While cfDNA shows promise as non-invasive biomarker for AMI, it is crucial that presence of other non-cardiac sources must be carefully considered. However, we cannot prevent the contribution of other major non-cardiac cfDNA sources like neutrophils but establishing a cardiac-specific methylation marker might reduce the influence of non-cardiac contributors. Futuristic approaches could involve developing algorithms that adjust for the high neutrophil contribution when analyzing cfDNA methylation, ensuring that cardiac-specific signals are not overshadowed by those from the immune response.

The differential methylation patterns observed in genes associated with the cAMP signaling pathway hold significant implications for the pathophysiology of AMI and potential therapeutic interventions. For instance, 5-hydroxytryptamine receptor 1A (HTR1A), a serotonin receptor hypomethylated in its promoter, may contribute to altered vascular tone and cardiac function during AMI. Increased serotonin levels during AMI have been reported previously [52] and could potentially trigger elevated expression of HTR1A receptors. Epigenetic mechanisms, such as promoter hypomethylation, may govern this heightened expression. Pharmacological activation of HTR1A receptors has shown promise in improving survival chances after cardiac arrest, highlighting the therapeutic potential of targeting this pathway [52].

Similarly, differential methylation in genes encoding G protein-coupled receptors (GPCRs) involved in the cAMP signaling pathway, such as GHSR and FFAR2, underscores the importance of epigenetic regulation in cardiovascular health.

GHSR, which acts as a receptor for ghrelin and is expressed in cardiac tissue, demonstrates cardioprotective properties. Ghrelin emerges as a promising candidate for cardiovascular disease treatment [53]. The observed gene body hypermethylation in the GHSR gene in cfDNA confirms its regulatory function. Past studies have indicated reduced ghrelin levels and increased GHSR expression in heart failure patients, implying a potential mechanism for cardiac protection via GHSR overexpression [54]. While FFAR2 has been linked to modulating biological processes in response to changes in nutritional status and connecting dietary effects with cardiovascular health, its direct involvement in cardiovascular disease remains relatively unexplored. However, the observed differential methylation of FFAR2 in AMI patients implies its potential relevance to the condition [55]. Considering the importance of the FFAR2 as a signaling molecule in regulating the levels of blood glucose, inflammation, and lipids, Ruan et al. [56] reported its low expression in the peripheral blood of AMI patients compared to controls. Hence, low expression of FFAR2 has been regarded as an independent risk factor and a potential biomarker in the prediction of AMI.

The cardioprotective effects of the VIP signaling system, mediated by VIPR2, further highlight the intricate regulation of the cAMP signaling pathway in maintaining cardiac health. VIPR2 serves as the receptor molecule for VIP, a small 28-amino acid neuropeptide involved in the autonomic regulation of the cardiovascular system, exerting positive inotropic and chronotropic effects [57]. Hypomethylation of VIPR2 in the gene body indicates epigenetic regulation of this pathway, warranting further exploration of its role in AMI.

Additionally, differential methylation in genes such as ADCY9, NMDA receptor, and GRIN2D provides insights into the dysregulation of calcium signaling and

ion-exchange pathways during AMI, contributing to myocardial damage and cardiomyocyte apoptosis [58]. The multifaceted effects of these epigenetic changes within the cAMP signaling pathway and molecular interactions highlight a sophisticated and complex interplay that governs cardiac responses during and after AMI. Understanding these interactions could pave the way for innovative strategies to enhance recovery by identifying potential targets for therapeutic interventions and improving outcomes in AMI patients.

Despite our diligent efforts in study design, the study has certain limitations that we want to discuss here. We used methylation data from 25 AMI patients, but the comparison was made only in 14 patients for whom we obtained both cfDNA and gDNA methylation data. We acknowledge that a larger sample size could lead to robust conclusions. However, the current study focuses on intra-patient comparisons, thereby reducing the confounding variability typically introduced by external factors, which often necessitates a larger sample size. Additionally, the high depth and accuracy of molecular data from high-throughput sequencing allow us to detect subtle changes at the single-nucleotide level, making the smaller sample size adequate for this study. However, evaluating the study outcomes in a larger cohort would highlight the significance of cfDNA in AMI patients and offer a more thorough understanding of its potential as a biomarker for AMI.

We took utmost care in processing the blood samples swiftly and precisely for cfDNA. We have acknowledged various factors that may have influenced our findings and identified opportunities to improve the comprehensiveness and reliability of our study. While we could not entirely exclude the heterogeneity observed in cfDNA due to underlying pathologies in AMI patients, our deconvolution analysis includes 25 cell types, encompassing major organs and cell types. Nevertheless, incorporating more cell types in the analysis could enhance our understanding of cfDNA origins.

It is important to mention that we deliberately excluded gDNA methylation from healthy controls to focus on our primary objective of examining cfDNA behavior in AMI patients and its differences from gDNA methylation, though we considered using cfDNA from healthy adults as a comparator. However, due to the limited cfDNA yield from healthy individuals, we were unable to proceed with library preparation and global methylome sequencing within the ethical limits of blood collection. It is well known, and our findings align with this that cfDNA levels in healthy adults are significantly lower than in disease states. Nonetheless, Cuadrat et al. [46] successfully obtained cfDNA from healthy individuals and conducted methylation assays with as little as 10 ng of DNA. Therefore, expanding our study to compare methylation with cfDNA from healthy adults will provide a broader epigenetic insight.

Conclusion

The current study explored the global methylation profiles of cfDNA and gDNA obtained from AMI patients, aiming to identify their distinctive features and similarities. The noticeable stratification of methylation signatures between cfDNA and gDNA suggests the presence of specific epigenetic alterations associated with cfDNA, which could serve as diagnostic or prognostic indicators targeting these methylome signatures. Establishing a specific cfDNA methylation panel can improve diagnostic accuracy, support patient stratification, and help inform personalized treatment approaches. The identification of differentially methylated genes linked to cardiac muscle contraction, inflammation, hypoxia, and lipid metabolism underscores the potential of cfDNA to harbor disease-related information. Further validation of the epigenetic regulation at the transcriptome level is crucial to confirm the role of epigenetics influencing the pathophysiology of AMI. Complementary as well as follow-up studies are warranted to validate these findings by expanding the cohort size and comparing them to healthy controls.

Abbreviations

cfDNA	Cell-free DNA
ctDNA	Circulating tumor DNA
AMI	Acute myocardial infarction
ROS	Reactive oxygen species
NETs	Neutrophil extracellular traps
EPCs	Erythrocyte progenitor cells
cAMP	Cyclic adenosine monophosphate
HTR1A	5-Hydroxytryptamine receptor 1A
GPCRs	G protein-coupled receptors
GHSR	Ghrelin receptor
FFAR2	Free fatty acid receptor 2
VIP	Vasoactive intestinal peptide
VIPR2	Vasoactive intestinal peptide receptor 2
ADCY9	Adenylate cyclase 9
NMDA	N-methyl-D-aspartate
GRIN2D	Glutamate ionotropic receptor NMDA-type subunit 2D

Supplementary Information

The online version contains supplementary material available at https://doi.org/10.1186/s13148-024-01755-2.

Additional file1 (XLSX 46 KB)

Additional file2 (XLSX 118 KB)

Additional file3 (XLSX 20 KB)

Acknowledgements

The authors acknowledge the facilities provided by Central Molecular Laboratory, Govind Ballabh Pant Postgraduate Institute of Medical Education and Research (GIPMER), New Delhi, India.

Author contributions
B.M. and S.S.J. conceptualized the work. B.M., S.S.J., and M.D. conceived the experimental design of the study. G.M.D. collected and preprocessed the samples. G.M.D., A.K.S., and N. performed the library preparation and other wet-lab experiments. M.D., S.S., and P.S. handled data curation and conducted the bioinformatics analysis. M.D. and G.M.D. wrote the original draft. M.D., S.S., and G.M.D. generated the figures. B.M. and S.S.J. secured the funding, provided resources, and supervised the work. All authors reviewed and edited the manuscript and approved it for publication.

Funding
This work was supported by Department of Biotechnology (Grant ID: BT/INF/22/SP33063/2019) and Indian Council of Medical Research (Grant ID: ISRM/12(44)/2020), Government of India. The authors acknowledge the facilities provided by Central Molecular Laboratory, Govind Ballabh Pant Postgraduate Institute of Medical Education and Research (GIPMER), New Delhi, India.

Availability of data and materials
Methylome data generated by EM-Seq from this study were deposited to BioProject database under accession number PRJNA1153757 (https://www.ncbi.nlm.nih.gov/bioproject/?term=PRJNA1153757).

Declarations

Ethics approval and consent to participate
The study was approved by the Institute ethics committee (IEC/MAMC/(75/03/2020/No:116)) of Maulana Azad Medical College, New Delhi, INDIA.

Consent for publication
All patients included in the study provided their informed written consent after receiving comprehensive information about the study and its objectives.

Competing interests
The authors declare no competing interests.

Author details
[1]Central Molecular Laboratory, Govind Ballabh Pant Institute of Postgraduate Medical Education and Research (GIPMER), New Delhi, India. [2]School of Medicine, Center for Aging, Tulane University, Louisiana, USA. [3]Department of Biochemistry, Govind Ballabh Pant Institute of Postgraduate Medical Education and Research (GIPMER), Room No:419, Fourth Floor, Academic Block, New Delhi, India. [4]Department of GI Surgery, Govind Ballabh Pant Institute of Postgraduate Medical Education and Research (GIPMER), New Delhi, India.

Received: 29 August 2024 Accepted: 30 September 2024
Published online: 16 October 2024

References

1. Lindstrom M, DeCleene N, Dorsey H, Fuster V, Johnson CO, LeGrand KE, et al. Global burden of cardiovascular diseases and risks collaboration, 1990–2021. J Am Coll Cardiol. 2022;80:2372–425. https://doi.org/10.1016/j.jacc.2022.11.001.
2. Di Cesare M, Bixby H, Gaziano T, Hadeed L, Kabudula C, McGhie DV, et al. World Heart Report 2023: Confronting the world's number one killer. Geneva, Switzerland: World Heart Federation; 2023.
3. Wu P, Yu S, Wang J, Zou S, Yao D-S, Xiaochen Y. Global burden, trends, and inequalities of ischemic heart disease among young adults from 1990 to 2019: a population-based study. Front Cardiovasc Med. 2023;10:1274663. https://doi.org/10.3389/fcvm.2023.1274663.
4. Tamis-Holland JE, Jneid H, Reynolds HR, Agewall S, Brilakis ES, Brown TM, et al. Contemporary diagnosis and management of patients with myocardial infarction in the absence of obstructive coronary artery disease: a scientific statement from the american heart association. Circulation. 2019;139:e891-908. https://doi.org/10.1161/CIR.0000000000000670.
5. Winnige P, Vysoky R, Dosbaba F, Batalik L. Cardiac rehabilitation and its essential role in the secondary prevention of cardiovascular diseases. World J Clin Cases. 2021;9:1761–84. https://doi.org/10.12998/wjcc.v9.i8.1761.
6. Ho FK, Gray SR, Welsh P, Gill JMR, Sattar N, Pell JP, et al. Ethnic differences in cardiovascular risk: examining differential exposure and susceptibility to risk factors. BMC Med. 2022;20:149. https://doi.org/10.1186/s12916-022-02337-w.
7. Fu Z, Ma Y, Yang C, Liu Q, Liang J, Weng Z, et al. Association of air pollution exposure and increased coronary artery disease risk: the modifying effect of genetic susceptibility. Environ Health. 2023;22:85. https://doi.org/10.1186/s12940-023-01038-y.
8. Khera AV, Emdin CA, Drake I, Natarajan P, Bick AG, Cook NR, et al. Genetic risk, adherence to a healthy lifestyle, and coronary disease. N Engl J Med. 2016;375:2349–58. https://doi.org/10.1056/NEJMoa1605086.
9. McPherson R, Tybjaerg-Hansen A. Genetics of coronary artery disease. Circ Res. 2016;118:564–78. https://doi.org/10.1161/CIRCRESAHA.115.306566.
10. Lippi G, Cervellin G. The interplay between genetics, epigenetics and environment in modulating the risk of coronary heart disease. Ann Transl Med. 2016;4:460. https://doi.org/10.21037/atm.2016.12.29.
11. Wasim R, Mahmood T, Siddiqui MH, Singh A, Ahmad A, Ahsan F. Role of epigenetics in cardiovascular diseases: an out and out check. Intelligent Pharmacy. 2023;1:207–11. https://doi.org/10.1016/j.ipha.2023.09.001.
12. Cacabelos R. Pathoepigenetics: the role of epigenetic biomarkers in disease pathogenesis. Pharmacoepigenetics: Elsevier; 2019. p. 139–89. https://doi.org/10.1016/B978-0-12-813939-4.00005-X.
13. Shi Y, Zhang H, Huang S, Yin L, Wang F, Luo P, et al. Epigenetic regulation in cardiovascular disease: mechanisms and advances in clinical trials. Signal Transduct Target Ther. 2022;7:200. https://doi.org/10.1038/s41392-022-01055-2.
14. Sumi MP, Mahajan B, Sattar RSA, Nimisha, Apurva, Kumar A, et al. Elucidation of epigenetic landscape in coronary artery disease: a review on basic concept to personalized medicine. Epigenet Insights. 2021;14:2516865720988567. https://doi.org/10.1177/2516865720988567.
15. Agha G, Mendelson MM, Ward-Caviness CK, Joehanes R, Huan T, Gondalia R, et al. Blood leukocyte DNA methylation predicts risk of future myocardial infarction and coronary heart disease. Circulation. 2019;140:645–57. https://doi.org/10.1161/CIRCULATIONAHA.118.039357.
16. Fernández-Sanlés A, Sayols-Baixeras S, Subirana I, Sentí M, Pérez-Fernández S, de Castro MM, et al. DNA methylation biomarkers of myocardial infarction and cardiovascular disease. Clin Epigenetics. 2021;13:86. https://doi.org/10.1186/s13148-021-01078-6.
17. Ghose S, Ghosh S, Tanwar VS, Tolani P, Kutum R, Sharma A, et al. Investigating coronary artery disease methylome through targeted bisulfite sequencing. Gene. 2019;721:144107. https://doi.org/10.1016/j.gene.2019.144107.
18. Liu Q, Ma J, Deng H, Huang S-J, Rao J, Xu W-B, et al. Cardiac-specific methylation patterns of circulating DNA for identification of cardiomyocyte death. BMC Cardiovasc Disord. 2020;20:310. https://doi.org/10.1186/s12872-020-01587-x.
19. Alcaide M, Cheung M, Hillman J, Rassekh SR, Deyell RJ, Batist G, et al. Evaluating the quantity, quality and size distribution of cell-free DNA by multiplex droplet digital PCR. Sci Rep. 2020;10:12564. https://doi.org/10.1038/s41598-020-69432-x.
20. de Miranda FS, Barauna VG, Dos Santos L, Costa G, Vassallo PF, Campos LCG. Properties and application of cell-free DNA as a clinical biomarker. Int J Mol Sci. 2021. https://doi.org/10.3390/ijms22179110.
21. Lehmann-Werman R, Neiman D, Zemmour H, Moss J, Magenheim J, Vaknin-Dembinsky A, et al. Identification of tissue-specific cell death using methylation patterns of circulating DNA. Proc Natl Acad Sci USA. 2016;113:E1826–34. https://doi.org/10.1073/pnas.1519286113.
22. Dash M, Mahajan B, Dar GM, Sahu P, Saluja SS. An update on the cell-free DNA-derived methylome as a non-invasive biomarker for coronary artery disease. Int J Biochem Cell Biol. 2024;169:106555. https://doi.org/10.1016/j.biocel.2024.106555.
23. Mattox AK, Douville C, Wang Y, Popoli M, Ptak J, Silliman N, et al. The origin of highly elevated cell-free DNA in healthy individuals and patients with pancreatic, colorectal, lung, or ovarian cancer. Cancer Discov. 2023;13:2166–79. https://doi.org/10.1158/2159-8290.CD-21-1252.
24. Vaisvila R, Ponnaluri VKC, Sun Z, Langhorst BW, Saleh L, Guan S, et al. Enzymatic methyl sequencing detects DNA methylation at single-base

resolution from picograms of DNA. Genome Res. 2021;31:1280–9. https://doi.org/10.1101/gr.266551.120.
25. Merkel A, Fernández-Callejo M, Casals E, Marco-Sola S, Schuyler R, Gut IG, et al. gemBS: high throughput processing for DNA methylation data from bisulfite sequencing. Bioinformatics. 2019;35:737–42. https://doi.org/10.1093/bioinformatics/bty690.
26. Akalin A, Kormaksson M, Li S, Garrett-Bakelman FE, Figueroa ME, Melnick A, et al. methylKit: a comprehensive R package for the analysis of genome-wide DNA methylation profiles. Genome Biol. 2012;13:R87. https://doi.org/10.1186/gb-2012-13-10-r87.
27. Akalin A, Franke V, Vlahoviček K, Mason CE, Schübeler D. Genomation: a toolkit to summarize, annotate and visualize genomic intervals. Bioinformatics. 2015;31:1127–9. https://doi.org/10.1093/bioinformatics/btu775.
28. Wang Q, Li M, Wu T, Zhan L, Li L, Chen M, et al. Exploring epigenomic datasets by chipseeker. Curr Protoc. 2022;2:e585. https://doi.org/10.1002/cpz1.585.
29. Wu T, Hu E, Xu S, Chen M, Guo P, Dai Z, et al. clusterProfiler 4.0: a universal enrichment tool for interpreting omics data. Innovation (Camb). 2021;2:100141. https://doi.org/10.1016/j.xinn.2021.100141.
30. Ge SX, Jung D, Yao R. ShinyGO: a graphical gene-set enrichment tool for animals and plants. Bioinformatics. 2020;36:2628–9. https://doi.org/10.1093/bioinformatics/btz931.
31. Moss J, Magenheim J, Neiman D, Zemmour H, Loyfer N, Korach A, et al. Comprehensive human cell-type methylation atlas reveals origins of circulating cell-free DNA in health and disease. Nat Commun. 2018;9:5068. https://doi.org/10.1038/s41467-018-07466-6.
32. Bioconductor - deconvR n.d. https://bioconductor.org/packages/release/bioc/html/deconvR.html (Accessed May 1, 2024).
33. Krijnen PAJ, Nijmeijer R, Meijer CJLM, Visser CA, Hack CE, Niessen HWM. Apoptosis in myocardial ischaemia and infarction. J Clin Pathol. 2002;55:801–11. https://doi.org/10.1136/jcp.55.11.801.
34. Jjingo D, Conley AB, Yi SV, Lunyak VV, Jordan IK. On the presence and role of human gene-body DNA methylation. Oncotarget 2012;3:462–74. https://doi.org/10.18632/oncotarget.497.
35. Shayevitch R, Askayo D, Keydar I, Ast G. The importance of DNA methylation of exons on alternative splicing. RNA. 2018;24:1351–62. https://doi.org/10.1261/rna.064865.117.
36. Teissandier A, Bourc'his D. Gene body DNA methylation conspires with H3K36me3 to preclude aberrant transcription. EMBO J. 2017;36:1471–3. https://doi.org/10.15252/embj.201796812.
37. Le NT, Harukawa Y, Miura S, Boer D, Kawabe A, Saze H. Epigenetic regulation of spurious transcription initiation in arabidopsis. Nat Commun. 2020;11:3224. https://doi.org/10.1038/s41467-020-16951-w.
38. Telekes A, Horváth A. The role of cell-free DNA in cancer treatment decision making. Cancers (Basel). 2022. https://doi.org/10.3390/cancers14246115.
39. Adhit KK, Wanjari A, Menon S, Siddhaarth K. Liquid biopsy: an evolving paradigm for non-invasive disease diagnosis and monitoring in medicine. Cureus. 2023;15:e50176. https://doi.org/10.7759/cureus.50176.
40. Kumar S, Nguyen DT, Graviss EA, Patil S, Kim JH, Suarez EE, et al. (512) Donor-derived cell-free DNA in heart multiorgan transplantation. J Heart Lung Transplant. 2023;42:S233. https://doi.org/10.1016/j.healun.2023.02.527.
41. Obrișcă B, Butiu M, Sibulesky L, Bakthavatsalam R, Smith KD, Gimferrer I, et al. Combining donor-derived cell-free DNA and donor specific antibody testing as non-invasive biomarkers for rejection in kidney transplantation. Sci Rep. 2022;12:15061. https://doi.org/10.1038/s41598-022-19017-7.
42. Edwards RL, Menteer J, Lestz RM, Baxter-Lowe LA. Cell-free DNA as a solid-organ transplant biomarker: technologies and approaches. Biomark Med. 2022;16:401–15. https://doi.org/10.2217/bmm-2021-0968.
43. Tan E, Liu D, Perry L, Zhu J, Cid-Serra X, Deane A, et al. Cell-free DNA as a potential biomarker for acute myocardial infarction: a systematic review and meta-analysis. Int J Cardiol Heart Vasc. 2023;47:101246. https://doi.org/10.1016/j.ijcha.2023.101246.
44. Dong C, Chen J, Zheng J, Liang Y, Yu T, Liu Y, et al. 5-Hydroxymethylcytosine signatures in circulating cell-free DNA as diagnostic and predictive biomarkers for coronary artery disease. Clin Epigenetics. 2020;12:17. https://doi.org/10.1186/s13148-020-0810-2.
45. Zemmour H, Planer D, Magenheim J, Moss J, Neiman D, Gilon D, et al. Non-invasive detection of human cardiomyocyte death using methylation patterns of circulating DNA. Nat Commun. 2018;9:1443. https://doi.org/10.1038/s41467-018-03961-y.
46. Cuadrat RRC, Kratzer A, Arnal HG, Rathgeber AC, Wreczycka K, Blume A, et al. Cardiovascular disease biomarkers derived from circulating cell-free DNA methylation. NAR Genom Bioinform. 2023;5:lqad061. https://doi.org/10.1093/nargab/lqad061.
47. Ren J, Jiang L, Liu X, Liao Y, Zhao X, Tang F, et al. Heart-specific DNA methylation analysis in plasma for the investigation of myocardial damage. J Transl Med. 2022;20:36. https://doi.org/10.1186/s12967-022-03234-9.
48. Neri F, Rapelli S, Krepelova A, Incarnato D, Parlato C, Basile G, et al. Intragenic DNA methylation prevents spurious transcription initiation. Nature. 2017;543:72–7. https://doi.org/10.1038/nature21373.
49. Lokk K, Modhukur V, Rajashekar B, Märtens K, Mägi R, Kolde R, et al. DNA methylome profiling of human tissues identifies global and tissue-specific methylation patterns. Genome Biol. 2014;15:r54. https://doi.org/10.1186/gb-2014-15-4-r54.
50. Zhang S-C, Wang M-Y, Feng J-R, Chang Y, Ji S-R, Wu Y. Reversible promoter methylation determines fluctuating expression of acute phase proteins. ELife 2020;9. https://doi.org/10.7554/eLife.51317
51. Horckmans M, Ring L, Duchene J, Santovito D, Schloss MJ, Drechsler M, et al. Neutrophils orchestrate post-myocardial infarction healing by polarizing macrophages towards a reparative phenotype. Eur Heart J. 2017;38:187–97. https://doi.org/10.1093/eurheartj/ehw002.
52. Dreteler GH, Wouters W, Saxena PR. Comparison of the cardiovascular effects of the 5-HT1A receptor agonist flesinoxan with that of 8-OH-DPAT in the rat. Eur J Pharmacol. 1990;180:339–49. https://doi.org/10.1016/0014-2999(90)90319-2.
53. Mao Y, Tokudome T, Kishimoto I. Ghrelin as a treatment for cardiovascular diseases. Hypertension. 2014;64:450–4. https://doi.org/10.1161/HYPERTENSIONAHA.114.03726.
54. Beiras-Fernandez A, Kreth S, Weis F, Ledderose C, Pöttinger T, Dieguez C, et al. Altered myocardial expression of ghrelin and its receptor (GHSR-1a) in patients with severe heart failure. Peptides. 2010;31:2222–8. https://doi.org/10.1016/j.peptides.2010.08.019.
55. Richards LB, Li M, van Esch BCAM, Garssen J, Folkerts G. The effects of short-chain fatty acids on the cardiovascular system. PharmaNutrition. 2016;4:68–111. https://doi.org/10.1016/j.phanu.2016.02.001.
56. Ruan J, Meng H, Wang X, Chen W, Tian X, Meng F. Low expression of FFAR2 in peripheral white blood cells may be a genetic marker for early diagnosis of acute myocardial infarction. Cardiol Res Pract. 2020;2020:3108124. https://doi.org/10.1155/2020/3108124.
57. Henning RJ, Sawmiller DR. Vasoactive intestinal peptide: cardiovascular effects. Cardiovasc Res. 2001;49:27–37. https://doi.org/10.1016/S0008-6363(00)00229-7.
58. Liu Z-Y, Hu S, Zhong Q-W, Tian C-N, Ma H-M, Yu J-J. N-Methyl-D-aspartate receptor-driven calcium influx potentiates the adverse effects of myocardial ischemia-reperfusion injury ex vivo. J Cardiovasc Pharmacol. 2017;70:329–38. https://doi.org/10.1097/FJC.0000000000000527.

Publisher's Note